Toxicon 237 (2024) 107536

Contents lists available at ScienceDirect

Toxicon

journal homepage: www.elsevier.com/locate/toxicon

3-Epimers of Caribbean ciguatoxins in fish and algae

Elizabeth M. Mudge [a,*], Alison Robertson [b,c], Silvio Uhlig [d], Pearse McCarron [a], Christopher O. Miles [a,1]

[a] Biotoxin Metrology, National Research Council Canada, 1411 Oxford Street, Halifax, NS, B3H 3Z1, Canada
[b] Stokes School of Marine and Environmental Sciences, University of South Alabama, 600 Clinic Drive, Mobile, AL, 36688, USA
[c] Marine Ecotoxicology Lab, Dauphin Island Sea Lab, Dauphin Island, AL, 36528, USA
[d] Norwegian Veterinary Institute, P.O. Box 64, 1431, Ås, Norway

ARTICLE INFO

Handling editor: Ray Norton

Keywords:
Caribbean ciguatoxins
Borohydride reduction
C-CTX
LC−HRMS
Stereochemistry

ABSTRACT

Ciguatera poisoning (CP) is endemic to several subtropical and tropical regions and is caused by the consumption of fish contaminated with ciguatoxins (CTXs). The recent discovery of Caribbean CTXs (C-CTXs) in *Gambierdiscus* spp. isolated from the Caribbean resulted in the identification of a precursor analogue, C-CTX5, that is reduced into C-CTX1. C-CTX5 has two reducible sites, a ketone at C-3 and hemiketal at C-56. Chemical reductions of C-CTX5 into C-CTX3/4 resulted in two peaks in the LC−HRMS chromatograms with a ratio that differed markedly from that observed in fish extracts and the reduction of C-CTX1 isolated from fish. Reduction of C-CTX5 should have produced four diastereoisomers of C-CTX3/4, prompting a more detailed study of the reduction products. LC–HRMS with a slow gradient was used to separate and detect the four stereoisomers of C-CTX3/4, and to determine the distribution of these analogues in naturally contaminated fish tissues and following chemical reduction of isolated analogues. The results showed that in naturally contaminated fish tissues C-CTX1/2 is a mixture of two diastereoisomers at C-3 and that C-CTX3/4 is a mixture of two pairs of diastereoisomers at C-3 and C-56. The data suggests that there is variability in the enzymatic reduction at C-3 and C-56 of C-CTXs in reef fish, leading to variations in the ratios of the four stereoisomers. Based on these findings, a naming convention for C-CTXs is proposed which aligns with that used for Pacific CTX congeners and will aid in the identification of the structure and stereochemistry of the different CTX analogues.

1. Introduction

Ciguatera poisoning (CP) is caused by the consumption of ciguatoxin-contaminated fish. Ciguatoxins (CTXs) are produced in some species of *Gambierdiscus* which are consumed by reef herbivores and undergo trophic transfer into secondary and tertiary consumers such as reef-associated fish that are commonly linked to CP cases (World Health Organization, 2020).

CTXs are a class of large, neutral polyethers. There are three separate subclasses originally described based on geographical region, but there is increasing evidence of overlap in these regional distinctions (Loeffler et al., 2022; World Health Organization, 2020). Consequently, it has been proposed to classify CTXs based on backbone structures (World Health Organization, 2020). CTXs associated with the Pacific Ocean are the most widely studied, with over 20 analogues identified to date (Murata et al., 1990; Satake et al., 1993, 1996; Yasumoto et al., 2000). The algal precursors CTX3B/C and CTX4A/B are produced by the benthic dinoflagellate *Gambierdiscus polynesiensis* and metabolic biotransformation has been established using *in vitro* and *in vivo* studies (Chinain et al., 2010; Clausing et al., 2018; Ikehara et al., 2017). Caribbean CTXs (C-CTXs) have a different backbone structure from those associated with the Pacific region (Lewis et al., 1998). Over 12 putative C-CTXs have been reported in fish, with eight having been structurally characterized with varying degrees of certainty (Fig. 1) (Abraham et al., 2012; Estevez et al., 2023; Kryuchkov et al., 2020; Mudge et al., 2023; Pottier et al., 2002a), although only C-CTX1 has been confirmed by NMR spectroscopy (Lewis et al., 1998) due to the lack of other C-CTXs isolated in quantities sufficient for these analyses. A novel algal precursor, C-CTX5, has recently been discovered to be produced by *Gambierdiscus silvae* and *G. caribaeus* (Mudge et al., 2023) and *in vitro* biotransformation experiments confirmed C-CTX5 to be a precursor to the structurally elucidated analogues C-CTX1/2 and

* Corresponding author. National Research Council of Canada, 1411 Oxford Street, Halifax, NS, Canada.
E-mail address: elizabeth.mudge@nrc-cnrc.gc.ca (E.M. Mudge).
[1] Present address: Norwegian Veterinary Institute, P.O. Box 64, 1431 Ås, Norway.

https://doi.org/10.1016/j.toxicon.2023.107536
Received 16 October 2023; Received in revised form 21 November 2023; Accepted 21 November 2023
Available online 2 December 2023

C-CTX3/4.

Kryuchkov et al. (2020) performed a series of experiments to assess the structural characteristics of C-CTX3/4 in fish extracts, using a semi-purified C-CTX1 fraction, and confirmed C-CTX3/4 as the C-56-reduced form of C-CTX1/2. The chemical reduction led to two chromatographic peaks attributed to C-CTX3 and C-CTX4 with identical LC−HRMS/MS characteristics and a similar ratio to those detected in the fish. The structural assignments of C-CTX3 and -4 by Kryuchkov et al.,

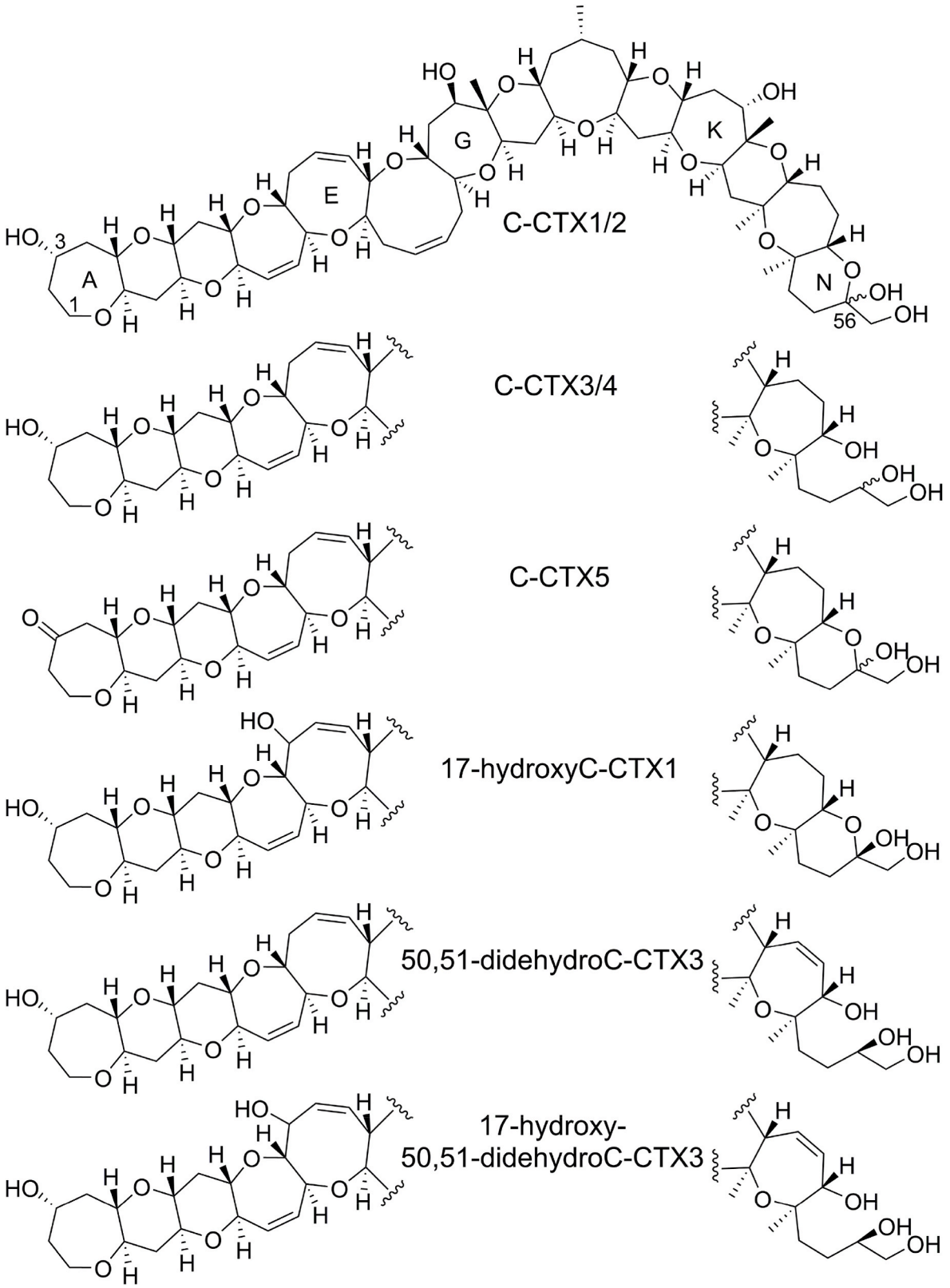

Fig. 1. Chemical structures of Caribbean ciguatoxins (C-CTXs) reported from fish and *Gambierdiscus* spp. Note: stereochemistry at C-56 is depicted as previously reported (Estevez et al., 2023; Kryuchkov et al., 2020; Lewis et al., 1998; Mudge et al., 2023).

(2020) were based on the published structure of C-CTX1 (Lewis et al., 1998). Following the identification of C-CTX5, which has a ketone at C-3, the same chemical reduction of C-CTX5 led to a ratio of C-CTX3/4 that differed significantly from that observed in *Sphyraena barracuda* (Mudge et al., 2023). Given the presence of two reducible sites for C-CTX5, that the $NaBH_4$ reduction should be repeatable, and that the C-56 position is too far from the 3-ketone group for either of them to influence the stereochemical outcome of the reduction of the other, this observed difference in C-CTX3/4 ratios was assumed to be due to the reduction of the C-3 ketone on C-CTX5 and warranted further investigation.

This study aimed to investigate the stereochemistry of C-CTX3/4 analogues produced during the chemical reduction of C-CTX5. Chromatographic conditions were modified to improve separation of the potential stereoisomers and experiments were monitored using HRMS. The methodology was then applied to naturally contaminated fish samples from a CP-endemic region to evaluate the distribution of C-CTX3/4 stereoisomers and to provide insight into the stereochemistry of C-CTX variants in nature. Similar chromatographic separations were performed for C-CTX1 and its 3-epimer using derivatized extracts from *G. silvae* and naturally contaminated fish.

2. Materials and methods

2.1. Reagents

Methanol, acetonitrile, formic acid (~98%), acetic acid (99%) were LC–MS grade from ThermoFisher Scientific (Ottawa, ON, Canada). Reagent grade sodium borohydride (>98%) and 0.22 μm PVDF spin filters were from Millipore–Sigma (Oakville, ON, Canada). Distilled water was ultra-purified to 18.2 MΩ × cm using a MilliQ purification system (Millipore–Sigma).

Methanolic extracts of fish collected from the 28th Bastille Day Kingfish Tournament (St. Thomas, U.S. Virgin Islands, USA) on July 17, 2016, were used as reference samples due to their verified presence of C-CTX1/2 and C-CTX3/4, and were prepared as described previously (Kryuchkov et al., 2020). This included four different *Sphyraena barracuda* (Great barracuda) and one *Scomberomorus regalis* (Cero mackerel) samples. *G. silvae* 1602 SH-6 methanolic extract, semi-purified C-CTX1/2 (from *Sphyraena barracuda* and *Scomberomorus cavalla*), C-CTX5 (from *G. silvae*), and C-CTX incubated microsome (*Archosargus probatocephalus*; T = 60 min) solutions were obtained as previously reported (Gwinn et al., 2021; Mudge et al., 2022, 2023). C-CTX1/2 from *G. silvae* was obtained as a side-fraction during the semi-purification of C-CTX5 (Mudge et al., 2023).

2.2. Sodium borohydride reduction

An aliquot (100 μL) of *G. silvae* 1602 SH-6 extract was evaporated to dryness under N_2 at 40 °C and redissolved in 50% MeOH (100 μL). Sodium borohydride (0.1 mg) was added and the sample was allowed to react for 15 min. Residual borohydride was hydrolyzed by the addition of acetic acid (2 μL), and analyzed by LC–HRMS.

An aliquot (20–100 μL) of the semi-purified C-CTX5, semi-purified C-CTX1/2 (from both fish and algae; prepared separately), and the sheepshead (*A. probatocephalus*) microsome T = 60 min solution, were evaporated to dryness under N_2 at 40 °C. The residues were redissolved in 50% MeOH (100 μL) and added to sodium borohydride (0.1 mg). The samples were allowed to react for 15 min and residual borohydride was hydrolyzed by the addition of acetic acid (2 μL), and analyzed by LC–HRMS.

2.3. C-CTX1 56-methyl ketal

Separate aliquots of *G. silvae* 1602 SH-6 (100 μL) and C-CTX-contaminated *S. barracuda* tissue methanolic extracts (DISL VIB16-42; 100 μL) were aliquoted, trifluoracetic acid (5 μL) was added, and the samples were allowed to react for 2 h at ambient temperature (Kryuchkov et al., 2022) and analyzed by LC−HRMS (Method 3).

2.4. LC–HRMS analysis

Analyses were performed using an Agilent 1290 Infinity II LC equipped with a binary pump, temperature controlled autosampler (10 °C) and temperature-controlled column compartment (Agilent Technologies, Missisauga, ON, Canada) coupled to a Q Exactive HF Orbitrap mass spectrometer (Thermo Fischer Scientific, Waltham, MA, USA) with a heated electrospray ionization probe (HESI-II). All methods employed gradient elution with mobile phases composed of H_2O (A) and MeCN (B) both containing 0.1% formic acid.

Method 1: Chromatographic separation was performed on a Kinetex F5 UHPLC column (100 × 2.1 mm, 1.7 μm; Phenomenex, Torrance, CA, USA) maintained at 40 °C. The gradient (0.3 mL/min) was: 0–18 min, 30–60% B; 18–18.1 min, 60–99% B; 18.1–22 min, 99% B; followed by an 8 min re-equilibration at 30% B.

Method 2: Chromatographic separation was performed on a Hypersil Gold C18 UHPLC column (100 × 2.1 mm, 1.9 μm; ThermoFisher Scientific, Waltham, MA, USA) maintained at 40 °C. The gradient (0.3 mL/min) was: 0–30 min, 32–41% B; 30–30.1 min, 41–99% B; 30.1–33 min, 99% B; followed by a 7 min re-equilibration at 32% B.

Method 3: Chromatographic separation was performed on a Hypersil Gold C18 UHPLC column (100 × 2.1 mm, 1.9 μm; ThermoFisher Scientific, Waltham, MA, USA) maintained at 30 °C. The gradient (0.3 mL/min) was: 0–40 min, 47–52% B; 40–40.1 min, 52–99% B; 40.1–43 min, 99% B; followed by a 7 min re-equilibration at 47% B.

Full-scan acquisition was performed with positive ionization with a mass range of *m/z* 1000–1250. The spray voltage of the source was +4.5 kV, with a capillary temperature of 340 °C. The sheath and auxiliary gas were set at 40 and 10 (arbitrary units). The auxiliary gas temperature was set at 150 °C and the S-Lens RF level was set to 100. The mass resolution setting was 120,000 with an automatic gain control (AGC) target of 3×10^6 and a maximum injection time of 250 ms per scan. Extracted-ion chromatograms were obtained with a mass tolerance of ±5 ppm. Product-ion spectra were acquired using parallel reaction monitoring (PRM) scan mode with an isolation window of 1 *m/z*. The resolution setting was 60,000 with an AGC target of 5×10^6 and a maximum injection time of 1000 ms with a normalized collision energy of 12 in positive mode.

Isomer ratios were estimated by fitting Gaussian peaks to the extracted-ion chromatograms using Fityk v1.3.1 (http://fityk.nieto.pl). In each chromatogram of C-CTX3/4, peak widths of the isomers were constrained to be identical. In the case of the methyl ketals of algal C-CTX1, the peak widths were additionally constrained to the value determined from analysis of the methyl ketals in the DISL-VIB16-42 sample.

3. Results and discussion

3.1. Borohydride reduction of C-CTX5

C-CTX5, identified as 3-oxo-C-CTX1/2, was reduced to C-CTX3/4 using sodium borohydride (Mudge et al., 2023). The reduction of the C-3 ketone moiety on C-CTX5 could potentially form two stereoisomers, along with the reduction of the N-ring hemiketal at C-56, and thus result in the formation of four stereoisomers (Fig. 2). Initial investigations using the LC−HRMS method 1, developed for improved detection of C-CTX1/2, only showed two main products (Fig. 3). This method used a pentafluorophenyl (F5) LC column, which improved peak shape and detection of C-CTX1/2 due to reduced interactions with the on-column, rapidly equilibrating epimers from the hemiketal at C-56 (Kryuchkov et al., 2020). However, this column did not separate the four isomers anticipated from $NaBH_4$-reduction of C-CTX5, even when isocratic

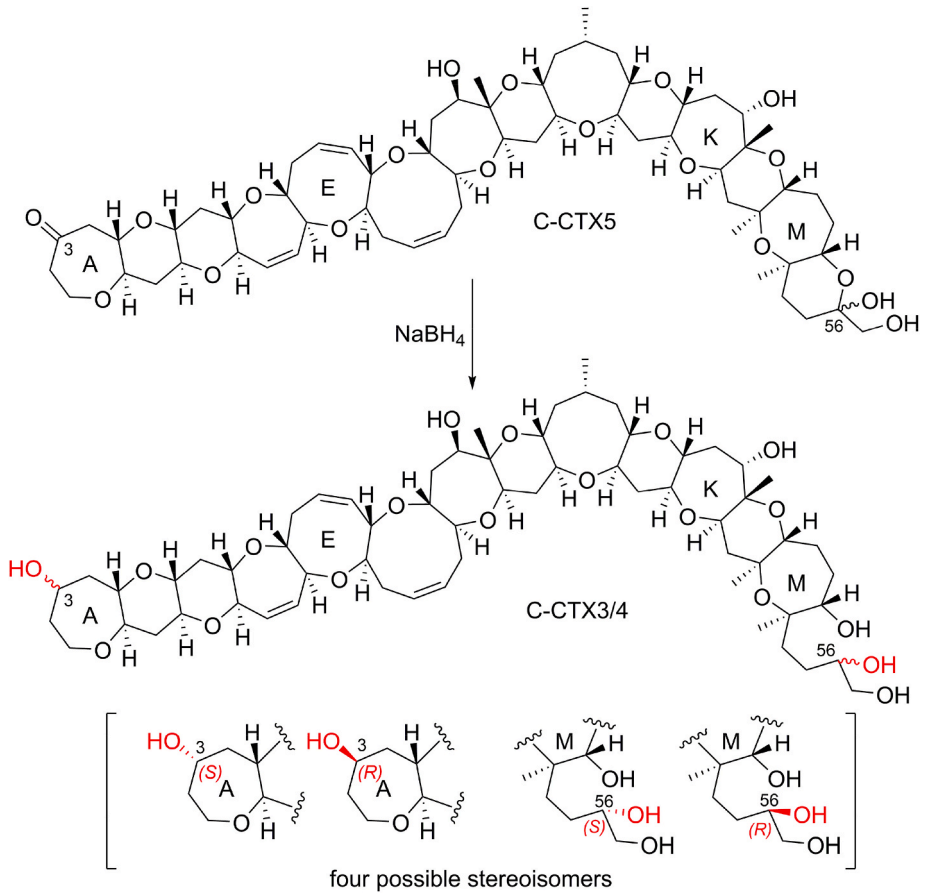

Fig. 2. Sodium borohydride reduction of C-CTX5, which reduces the C-3 ketone and C-56 hemi-ketal to produce four possible stereoisomers of C-CTX3/4.

conditions were employed. Additionally, chemical reduction of C-CTX5 resulted in a higher proportion of C-CTX4 relative to C-CTX3 than when C-CTX1 from fish was reduced. $NaBH_4$ should reproducibly reduce the C-56 hemiketal to a consistent ratio of stereoisomers. However, the ratio of C-CTX3/4 from C-CTX1 (reduced only at C-56) and C-CTX5 (reduced at C-3 and C-56) (Fig. 3), indicates that reduction at C-3 was responsible for this difference. This suggests co-elution of the four potential stereoisomers using chromatographic method 1, since only two peaks were observed.

3.2. LC–HRMS method for separation of C-CTX3/4 isomers

In order to chromatographically resolve the expected C-CTX3/4 isomers, a reversed-phase C18 column was used with a slow gradient (Method 2). Under these conditions, the first peak (C-CTX3) eluted after 17 min and all four isomers from the $NaBH_4$ reduced C-CTX5 sample could be detected (Fig. 4; top trace). This confirmed that there were indeed four stereoisomers of C-CTX3/4 produced by the reduction of C-CTX5. The separation resulted in two pairs of partially resolved peaks. Using peak deconvolution software, it was determined that the ratio of the areas of the first peak and the second peak within each pair was approximately 55:45 for both sets of peaks (Table S1, Fig. S1). Additional experiments were performed to assign the structures of the four peaks.

Samples containing semi-purified C-CTX5 and/or C-CTX1/2 from various sources were chemically reduced using sodium borohydride to produce C-CTX3/4 stereoisomers (Fig. 4). In all chemically-reduced samples, the ratio of the areas of the first peak to the second peak within a pair was consistently 55:45 using peak fitting estimates (Fig. S1; Table S1). The ratios of the areas of the first and second pairs of peaks from the reduction of semi-purified C-CTX5 and C-CTX1 from *G. silvae* varied significantly, where the second pair of peaks was more abundant than the first pair, while the reduction of C-CTX1 semi-purified from fish resulted in a high proportion of the first pair of peaks. A remaining sample of C-CTX5 that had been enzymatically converted to C-CTX1/2 using fish liver microsomes (Mudge et al., 2023), which contained approximately 80% C-CTX1/2 and 20% C-CTX5, was also reduced with $NaBH_4$. This resulted in a C-CTX3/4 stereochemical profile much closer to that observed with $NaBH_4$ reduced C-CTX1/2 from fish, where the first pair of peaks dominated the profile. Given that $NaBH_4$ should reduce at each position (C-3 and C-56) with a consistent ratio, and that a consistent ratio of 55:45 was observed between the peaks within a pair but not between the baseline-resolved peak pairs, strongly suggests that the peaks within a pair differ in their C-56 stereochemistry. Therefore, the baseline-resolved peaks are the 3-epimers, rather than the C-56 epimers originally proposed by Kryuchkov et al. (2020).

Product-ion spectra for the four C-CTX3/4 stereoisomers ($[M + H]^+$ at *m/z* 1143.6) indicated slight variations in the relative proportions of the low-mass product-ions when comparing the two peaks within a pair (Fig. 5). The first peak had a slightly higher relative intensity of the product ion *m/z* 283.1900 compared with the product ion at *m/z* 255.1587. For the second peak within a pair, the opposite relative proportion of these two product-ions was observed, where the *m/z* 255.1587 was higher than *m/z* 283.1898. These relative ratios were consistent when comparing the product-ion spectra of the second pair of peaks (Fig. S2). The fragmentation of C-CTX3/4 described by Kryuchkov et al. (2020) notes that these two product ions arise from cleavages between rings K–L and are indicative of the reduced N-ring hemiketal. This was confirmed from the product-ion spectrum of $NaBD_4$-reduced C-CTX1/2, where these product-ions were observed with an *m/z* consistent with the addition of one deuterium on the reduced hemiketal at C-56 (Fig. S3). Based on this, it appears that the variation in the

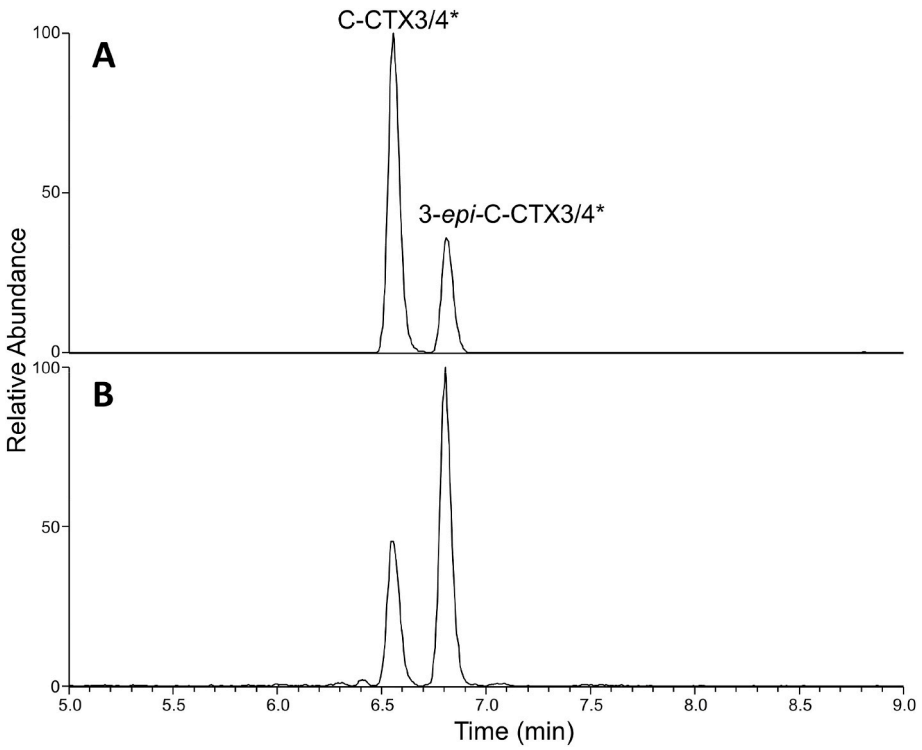

Fig. 3. Extracted-ion chromatograms of C-CTX3/4 ($[M + H]^+$ at *m/z* 1143.6462) using LC−HRMS Method 1, (A) C-CTX positive fish (*Sphyraena barracuda*) from St. Thomas, Virgin Islands and; (B) sodium borohydride reduced C-CTX5 (the algal precursor of C-CTX1) isolated from *G. silvae* to produce C-CTX3/4. The identities of the peaks are labeled based on the findings described herein. * Note that the first peak was originally ascribed to C-CTX3 and the second to C-CTX4 (with varying stereochemistry at C-56) by Kryuchkov et al. (2020).

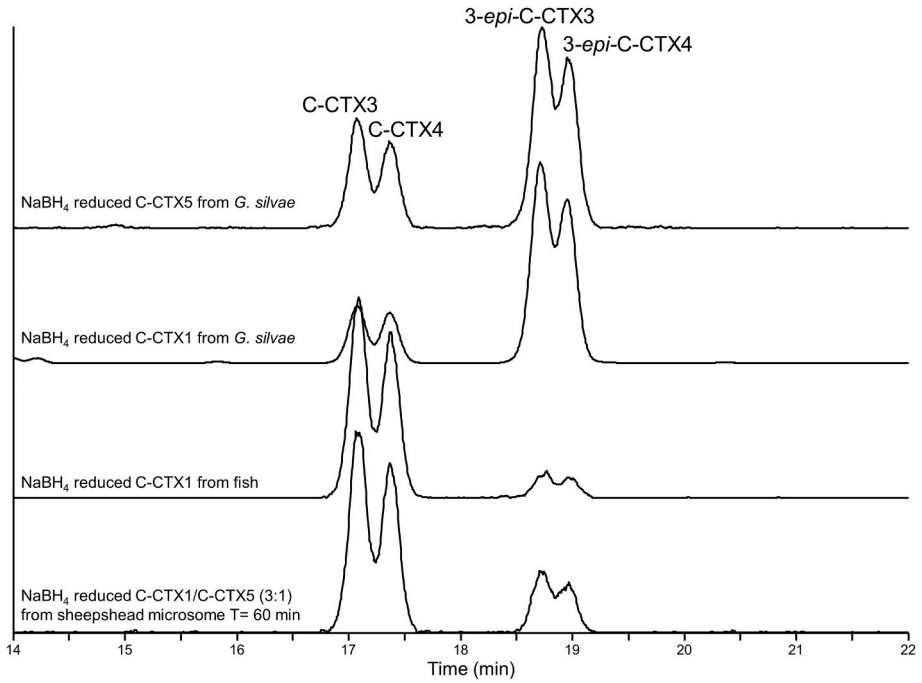

Fig. 4. Extracted-ion chromatogram of *m/z* 1143.6462 for C-CTX3/4 diastereoisomers after sodium borohydride reduction of semi-purified fractions of C-CTX5 and/or C-CTX1 from various sources (Method 2).

relative ratios of those product-ions is due to the stereochemistry of the C-56 diol, and further confirms that the two peaks within a pair differ in their stereochemistry at C-56. Based on this and the additional data presented below, it was concluded that the first set of peaks are the 56-epimers: C-CTX3 and C-CTX4, and the second set of peaks are their 3-epimers: 3-*epi*-C-CTX3 and 3-*epi*-C-CTX4 as labeled in Fig. 4.

3.3. Variation of C-CTX3/4 isomers in various fish

The variation in the proportion of the C-CTX3/4 isomers in five

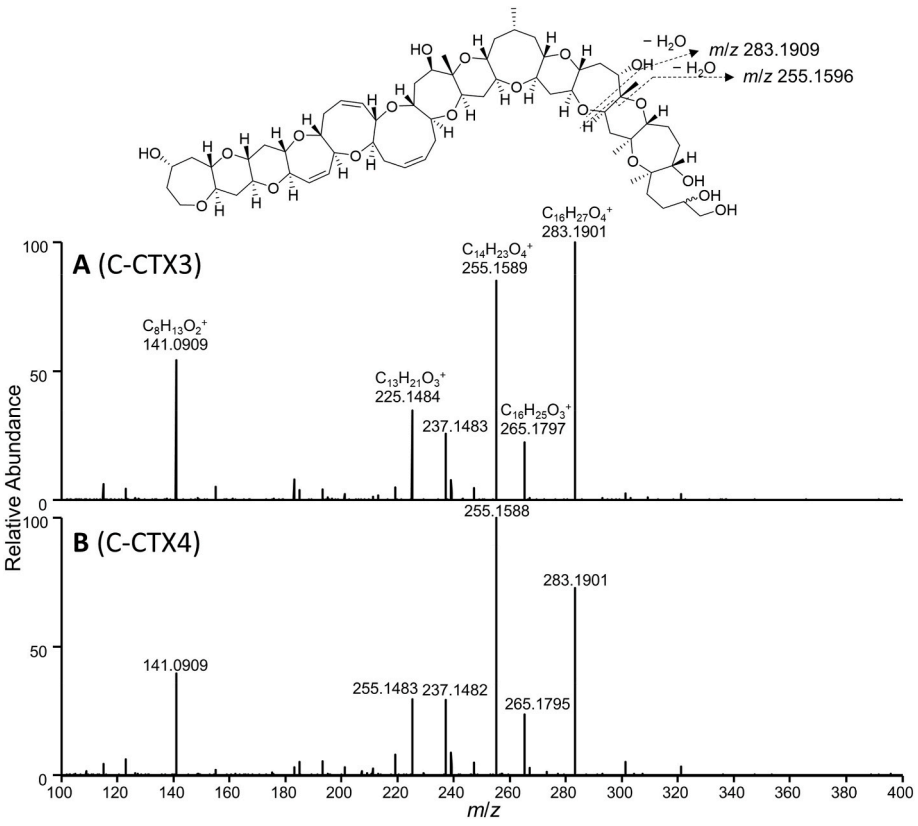

Fig. 5. Product-ion spectra of the first pair of partially resolved peaks: (A) C-CTX3 and (B) C-CTX4 as labeled in Fig. 4 with an $[M + H]^+$ at *m/z* 1143.6, displaying *m/z* 100 to 400 with the cleavages described as per Kryuchkov et al. (2020).

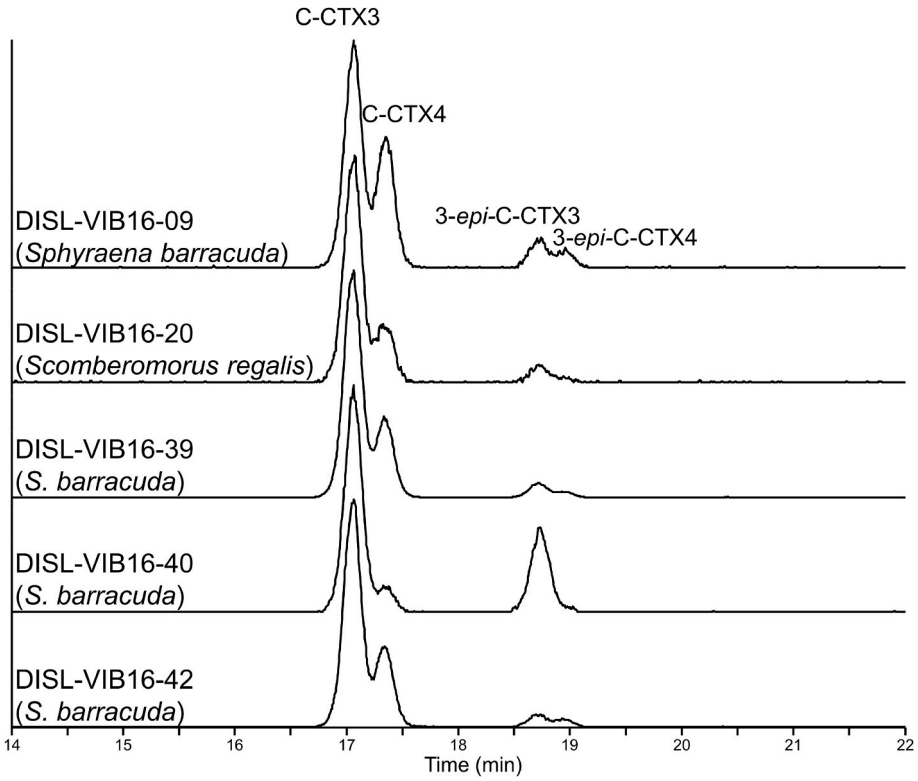

Fig. 6. LC−HRMS extracted-ion chromatogram of C-CTX3/4 ($[M + H]^+$ at *m/z* 1143.6462) in extracts of five naturally contaminated fish tissues (Method 2).

naturally contaminated ciguatoxic fish samples is summarized in Fig. 6. There was a much higher proportion of C-CTX3/4 than 3-*epi*-C-CTX3/4 in all samples examined, although the relative ratios of the two varied between samples (Table S2). Additionally, C-CTX3 was consistently the most abundant isomer. The ratios of the C-56 epimers was similar within an individual fish sample, but variable between individuals, where DISL-VIB16-9 had the lowest ratio at 63:37, while DISL-VIB16-40 had the highest ratio at 90:10. In contrast, DISL-VIB16-40 also had the lowest C-CTX3/4:3-*epi*-C-CTX3/4 ratio of 73:27, indicating that there is significant variation in the enzymatic specificity of the conversion to these reduced CTXs (Table S2). This suggests that the majority of C-CTX1/2 and C-CTX3/4 observed in the fish extracts may have been consumed as the algal precursor C-CTX5, and then enzymatically reduced in a stereoselective manner into the isomers dominating the toxin profiles in fish. Additionally, the variations in ratios could be the result of marine food web transfer involving different primary and secondary consumers.

3.4. C-CTX1 stereochemistry following methyl ketal formation

Chromatographic separation of C-CTX1 resulted in a broad peak due to on-column epimerization at C-56 (Kryuchkov et al., 2020). In order to eliminate this behaviour, the toxin was converted to the 56-methyl ketal by the addition of acid in methanol (Estevez et al., 2020; Kryuchkov et al., 2022). This produces a sharp chromatographic peak, therefore eliminating on-column epimerization, but LC−HRMS method 1 only resulted in a single peak (Kryuchkov et al., 2022). A slow gradient (method 3) was used to separate the expected C-3 epimers of C-CTX1 56-methyl ketal in aliquots of *G. silvae* 1602 SH-6 and DISL-VIB16-42 (Fig. 7). While baseline separation between the two epimers was not achieved, the chromatographic trace of the *G. silvae* extract resulted in two apices with a much broader peak than for the C-CTX contaminated fish extract. There is a very small amount of tailing observed for the fish extract consistent with the presence of the later-eluting C-3 epimer at a much lower proportion compared to the dominant earlier eluting epimer. Analysis with peak deconvolution software revealed the presence of the two peaks, and further confirmed that 3-*epi*-C-CTX1 occurs in natural samples of both reef fish and algae (Fig. S4). A *G. silvae* extract was used to prepare the methyl ketal, therefore direct comparison with the $NaBH_4$ reduced semi-purified C-CTX1/2 from algae cannot be made. However, the ratio of the 3-epimers of C-CTX1 in DISL-VIB16-42 (95:5) was very similar to the ratio of C-CTX3/4 to 3-*epi*-C-CTX3/4 (Table S2).

3.5. Stereochemistry assignment at C-3

The published structure of C-CTX1 by Lewis et al. (1998) identified the C-3 hydroxy group as α-oriented (3*S*) when isolated from *Caranx latus* collected from St. Barthelemy in the Caribbean Sea. Given that there is no remaining material available of this originally isolated C-CTX1 analogue, isolated more than 25 years ago, it is not possible to make direct comparisons with the fish tissues evaluated here. However, the consistent ratio of the 3-epimers of both C-CTX1 and C-CTX3/4 in DISL-VIB-42 strongly suggests that the 3-OH stereochemistry is conserved and there is a higher proportion of 3*S* C-CTX1 in fish. Additionally, the stereochemistry of C-CTX3/4 (3*S*) represents 73–93% of the C-CTX3/4:3-epi-C-CTX3/4 profile (Table S2) and is further supported by similar dominance of the C-CTX3 isomer in various fish species from the Canary Islands and Madeira archipelago (Estevez et al., 2023). Therefore, the isolated C-CTX1 was most likely a mixture of the two stereoisomers, but with greater than 90% having the 3*S* stereochemistry. The lower abundance of the 3*R*-epimer (<10%) would have impeded its analysis in the original NMR study (Lewis et al., 1998). This also strongly suggests that the C-3 stereochemistry of C-CTX3 is α-oriented (3*S*), while 3-*epi*-C-CTX3 is 3*R*.

3.6. Consideration of C-CTX stereochemistry in CP monitoring and research

This research on C-CTX stereochemistry was initiated when only two

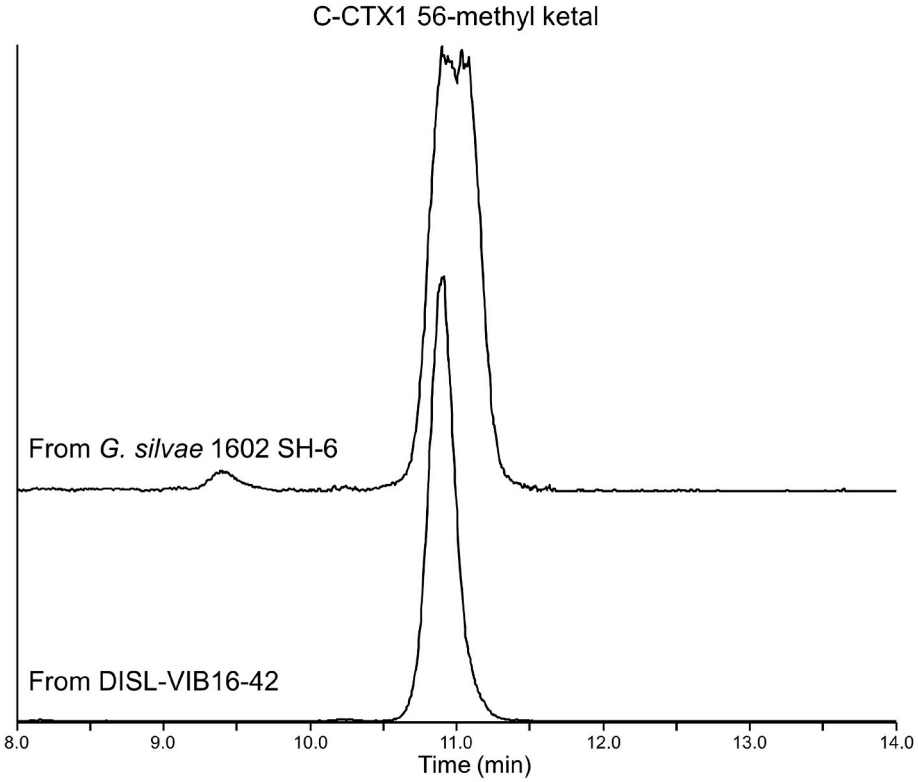

Fig. 7. LC−HRMS (Method 3) extracted-ion chromatogram of C-CTX1 56-methyl ketal ($[M + H - CH_3OH]^+$ at *m/z* 1123.6200) prepared from: top, C-CTX1 in *G. silvae* 1602 SH-6, and; bottom, naturally contaminated *S. barracuda* tissue (DISL-VIB16-42).

of the four anticipated stereoisomers were detected following the reduction of C-CTX5 with $NaBH_4$, and when it was observed that the ratio of the C-CTX5 reduction products differed markedly from those produced following reduction of C-CTX1. The resulting observation of four stereoisomers of C-CTX3/4 in extracts of naturally contaminated fish tissue expands our knowledge on the chemistry of C-CTXs in fish implicated in CP. In this work a slow LC gradient and long chromatographic run time was used to separate the four stereoisomers, which would not be conducive to the type high-throughput analyses generally employed for CTX screening and monitoring applications. However, the presence of these stereoisomers should be considered when establishing methods and data analysis processes.

Stereochemistry can significantly affect the binding affinity of marine toxins to the receptors associated with their toxicological effects, such as the C-11 stereoisomers of saxitoxin analogues on sodium channels (Leal and Cristiano, 2022) or the C-35 stereochemistry of dinophysistoxin-1 and dinophysistoxin-2 binding to protein phosphatases (Larsen et al., 2007). Thus, it is possible that the toxicities of C-CTX analogues are affected by both their C-3 and C-56 stereochemistries. The variations in the four C-CTX3/4 stereoisomer ratios in the naturally contaminated fish suggests that the ratios of the C-3 epimers of C-CTX1, the most abundant C-CTX in fish, is also variable between individual fish. These differences in stereoisomer abundance may also modify the toxicokinetics, binding affinities, half-lives, and metabolism, which may influence the toxicological effects. Future studies will be necessary to compare the effects of C-CTX stereochemistries on toxicology and metabolism.

Comparison of the $NaBH_4$-reduced C-CTX3/4 ratios to those observed in fish suggests that the chemical reduction favors a different ratio of stereoisomers than the enzymatic conversion. The variation between enzymatically- and chemically-reduced analogues will be important when considering the use of algal sources and reduction procedures to produce reference materials. Given the current limitations with C-CTX reference materials, the use of chemical reducing agents to produce C-CTX1 and/or C-CTX3/4 analogues from the algal precursor is an approach that will be considered in efforts to make reference materials available. However, this may result in stereoisomer proportions that do not reflect the natural distribution observed in fish. Therefore, if research shows that stereochemistry has a significant bearing on toxicology or metabolism, further work will be required to establish methods using enzymes or stereoselective reducing agents to produce profiles that more closely match those observed in nature.

These results reveal an unexpected diversity in the natural distribution of C-CTX analogues, but also suggest the dominance of the 3*S* stereoisomer in piscivorous reef fish. The data presented suggests that 3-OH C-CTXs, such as those reported by Estevez et al. (2023), are almost certain to occur as a mixture of 3-epimers, similar to that observed for the C-CTXs described here. Future work will need to be performed to understand the enzymatic conversion of C-CTXs by different fish species and *Gambierdiscus* spp. to gain a better insight into the factors influencing toxin profiles of natural samples.

3.7. Proposed naming convention for C-CTXs

Until the discovery of C-CTX5, it was unknown that C-CTX1 and other C-CTX analogues originated from an algal precursor with a C-3 ketone, which when reduced led to C-CTX1 and other analogues that could occur as stereoisomers. The identity of other C-CTXs was presumed through LC−HRMS/MS combined with chemical reactions, based on the published structure of C-CTX1. The data presented here describing the stereochemical diversity of C-CTXs suggests the need to standardize the naming conventions for C-CTXs to identify the structural characteristics of the analogues in a similar way to those used to describe CTX4A and CTX3C analogues.

Based on published NMR assignments by Lewis et al. (1998), C-CTX1 is the 3*S* analogue with a hemiketal at C-56, and C-CTX2 was considered to be the 56-epimer of C-CTX1. This hemiketal is now understood to undergo on-column equilibration and the pair of equilibrating epimers have been denoted as a single peak containing a mixture of C-CTX1/2 (Kryuchkov et al., 2020; Mudge et al., 2022, 2023). However, in-depth examination of the original C-CTX publications reveals several important considerations. Firstly, there was baseline separation between the elution of C-CTX1 and C-CTX2 by several minutes (Pottier et al., 2002a); secondly, formation of C-CTX2 occurred only in methanol (Pottier et al., 2002a, 2002b), but not in acetonitrile-based solvents (Lewis et al., 1998), and; thirdly, C-CTX2 converted back to C-CTX1 in MeCN–H_2O (Lewis et al., 1998). This suggests that the original compound denoted as C-CTX2 was likely C-CTX1 56-methyl ketal, which as described previously elutes several minutes later than C-CTX1 on reversed phase columns and with an MS spectrum dominated by the $[M + H - CH_3OH]^+$, which is essentially identical to that of C-CTX1 (Estevez et al., 2020; Kryuchkov et al., 2022). The published data shows that C-CTX1 56-methyl ketal is an artifact produced during the extraction and clean-up of CTXs when using methanol as an extraction solvent (Estevez et al., 2020; Kryuchkov et al., 2022). Given that recent publications do not separate the C-56 epimers of C-CTX1/2, it would seem reasonable to consider any C-CTXs with a C-56 hemiketal that undergoes rapid on-column epimerization and does not separate chromatographically as a single CTX analogue. Due to the historical naming of C-CTX2 (ie. 56-*epi*-C-CTX1), which appears to probably have been C-CTX1 56-methyl ketal, it should remain as C-CTX2 (56-*epi*-C-CTX1). However, it should be noted that it is not currently possible to chromatographically separate C-CTX2 from C-CTX1 and the two epimers appear to equilibrate very readily under acidic conditions. Therefore, we suggest referring to C-CTX1 and C-CTX2 collectively as C-CTX1 except in circumstances where the two 56-epimers need to be considered separately.

The results presented here revealed the presence of a 3-epimer of C-CTX1 with 3*R* stereochemistry in extracts of fish tissues and algae. 3-*epi*-C-CTX1 appears to be much more abundant in algae than in fish (Fig. 7; Fig. S4). However, it should be noted that this is based on comparison between a single algal extract and fish extract (DISL-VIB16-42). Unfortunately, it is not possible to separate the 3-epimers of C-CTX1 using a simple chromatographic separation, and only partial separation was achieved following conversion to their 56-methyl ketals. Therefore, at this stage it is only possible to note that 3-*epi*-C-CTX1 occurs naturally, although the distribution and its relative abundance in fish and microalgae is not yet well understood. Preliminary evidence comparing the 3-epimers (3*S*:3*R*) in DISL-VIB16-42 for C-CTX1 and C-CTX3/4, which were both approximately 94:6, suggests that the stereochemistry may be conserved across C-CTX variants in individual fish and that the C-CTX3/4:3-*epi*-C-CTX3/4 profile could be used as a proxy for the distribution of 3-*epi*-C-CTX1.

For the C-CTX3/4 analogues, it is evident that four stereoisomers exist in nature and can be chromatographically separated. Based on the evidence presented here, the two main peaks detected using faster gradient conditions vary in their C-3 stereochemistries and are described as C-CTX3/4 and 3-*epi*-C-CTX3/4, respectively. This peak identification is a correction from those described previously (Kryuchkov et al., 2020; Mudge et al., 2023), now that it is established that these vary in their C-3 stereochemistries. C-CTX3 and C-CTX4 are the C-56 epimers following reduction of the N-ring hemiketal with the 3*S* stereochemistry of the hydroxyl group. It is not possible to definitively assign which peak corresponds to which stereochemistry at C-56, but stereochemistry is tentatively assigned based on the original C-56 assignment of C-CTX1 (Lewis et al., 1998). C-CTX4 can also be referred to as 56-*epi*-C-CTX3. The same is true for the 3-*epi*-C-CTX3/4 stereoisomers (3*R*), where 3-*epi*-C-CTX4 is equivalent to 3-*epi*-56-*epi*-C-CTX3. Future work will be required to determine the 56-stereochemistry of one of the four C-CTX3/4 stereoisomers in order to fully define the peak assignments relating to the stereochemistry of this group of C-CTX metabolites. A summary of the suggested naming convention and structural variations for C-CTX1–5 is presented in Table 1.

Table 1
Proposed naming convention for C-CTXs based on the identification of C-CTX stereoisomers described herein. C-3 and C-56 assignments for C-CTX1 based on Lewis et al. (1998) *C-3 and C-56 assignments proposed based on structure of C-CTX1.

C-CTX	Descriptive nomenclature	A–B rings	M–N rings
C-CTX1[a]	C-CTX1	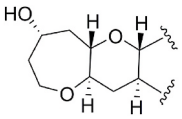	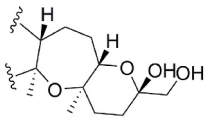
3-*epi*-C-CTX1	3-*epi*-C-CTX1	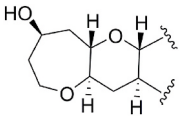	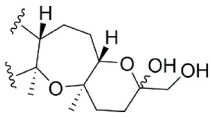
C-CTX2[a]	56-*epi*-C-CTX1	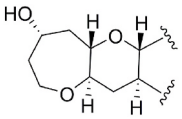	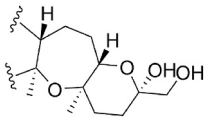
C-CTX1 56-methyl ketal[b]	C-CTX1 56-methyl ketal Previous names: 56-methoxyC-CTX1 C-CTX1-Me	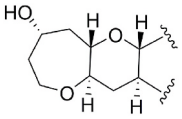	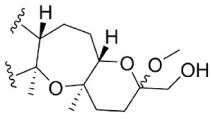
C-CTX3	C-CTX3	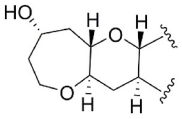	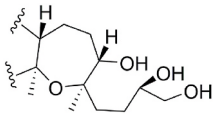
C-CTX4	56-*epi*-C-CTX3	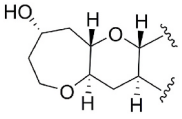	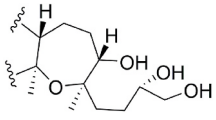
3-*epi*-C-CTX3	3-*epi*-C-CTX3	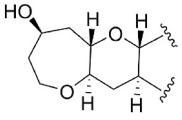	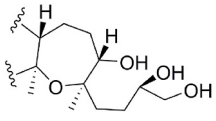
3-*epi*-C-CTX4	3-*epi*-C-CTX4 3-*epi*-56-*epi*-C-CTX3	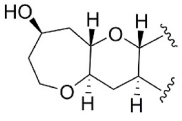	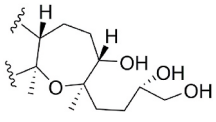
C-CTX5	C-CTX5 3-oxo-C-CTX1	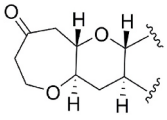	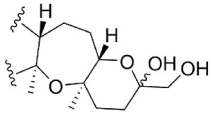

[a] Collectively, C-CTX1 and C-CTX2 can be referred to as C-CTX1 unless the two 56-epimers can be chromatographically separated.
[b] C-CTX1 56-methyl ketal is an artifact from extraction.

Credit author statement

Conceptualization, E.M.M. and C.O.M.; methodology, E.M.M. and C.O.M.; formal analysis, E.M.M.; investigation, E.M.M.; resources, A.R, S.U. and P.M.; writing—original draft preparation, E.M.M.; writing—review and editing, All Authors; supervision, P.M.; funding acquisition, A.R, C.O.M and P.M. All authors have read and agreed to the published version of the manuscript.

Ethical statement

The authors declare that they followed the ethics outlined in the Elsevier 'Publishing Ethics' Policies.

Declaration of competing interest

The authors declare that they have no known competing financial interests or personal relationships that could have appeared to influence the work reported in this paper.

Data availability

Data will be made available on request.

Acknowledgments

This research was funded by National Science Foundation (NSF) Partnerships in International Research and Education Program (CiguaPIRE; 1743802 to AR) and the Research Council of Norway (Grant No. 279247 to SU). This work also contributes to the NIH-NSF funded Greater Caribbean Center for Ciguatera Research (NIH: P01ES028949; NSF: 1841811 to AR).

The authors thank Tyler B. Smith (University of the Virgin Islands) and Deana L. Erdner (University of Texas Marine Sciences Institute) and their lab personnel for the original collection of live algal material, and *G. silvae* identification and culture establishment, respectively. We thank Katherine L. Baltzer (Dauphin Island Sea Lab) and Jessica K. Gwinn (University of South Alabama, Mobile, AL, USA) for assisting with collections at the 2016 Bastille Day Kingfish Tournament, and Clayton T. Bennett and Alexander K. Leynse (University of South Alabama) for technical support in the large-scale toxin extractions from *S. barracuda* and *S. regalis* used in this study. We thank Fedor Kryuchkov (Norwegian Veterinary Institute, Ås, Norway) who performed preliminary C-CTX profiling in prior Bastille Day fish tissues by LC−HRMS.

Appendix A. Supplementary data

Supplementary data to this article can be found online at https://doi.org/10.1016/j.toxicon.2023.107536.

References

Abraham, A., Jester, E.L.E., Granade, H.R., Plakas, S.M., Dickey, R.W., 2012. Caribbean ciguatoxin profile in raw and cooked fish implicated in ciguatera. Food Chem. 131, 192–198.

Chinain, M., Darius, H.T., Ung, A., Cruchet, P., Wang, Z., Ponton, D., Laurent, D., Pauillac, S., 2010. Growth and toxin production in the ciguatera-causing dinoflagellate *Gambierdiscus polynesiensis* (Dinophyceae) in culture. Toxicon 56, 739–750.

Clausing, R.J., Losen, B., Oberhaensli, F.R., Darius, H.T., Sibat, M., Hess, P., Swarzenski, P.W., Chinain, M., Dechraoui Bottein, M.-Y., 2018. Experimental evidence of dietary ciguatoxin accumulation in an herbivorous coral reef fish. Aquat. Toxicol. 200, 257–265.

Estevez, P., Leao, J.M., Yasumoto, T., Dickey, R.W., Gago-Martinez, A., 2020. Caribbean ciguatoxin-1 stability under strongly acidic conditions: characterisation of a new C-CTX1 methoxy congener. Food Addit. Contam. 37, 519–529.

Estevez, P., Oses Prieto, J., Burlingame, A., Gago Martinez, A., 2023. Characterization of the ciguatoxin profile in fish samples from the eastern Atlantic Ocean using capillary liquid chromatography−high resolution mass spectrometry. Food Chem. 418, 135960.

Gwinn, J.K., Uhlig, S., Ivanova, L., Fæste, C.K., Kryuchkov, F., Robertson, A., 2021. In vitro glucuronidation of Caribbean ciguatoxins in fish: first report of conjugative ciguatoxin metabolites. Chem. Res. Toxicol. 34, 1910–1925.

Ikehara, T., Kuniyoshi, K., Oshiro, N., Yasumoto, T., 2017. Biooxidation of ciguatoxins leads to species-specific toxin profiles. Toxins 9, 205.

Kryuchkov, F., Robertson, A., Miles, C.O., Mudge, E.M., Uhlig, S., 2020. LC–HRMS and chemical derivatization strategies for the structure elucidation of Caribbean ciguatoxins: identification of C-CTX-3 and -4. Mar. Drugs 18, 182.

Kryuchkov, F., Robertson, A., Mudge, E.M., Miles, C.O., Van Gothem, S., Uhlig, S., 2022. Reductive amination for LC–MS signal enhancement and confirmation of the presence of Caribbean ciguatoxin-1 in fish. Toxins 14, 399.

Larsen, K., Petersen, D., Wilkins, A.L., Samdal, I.A., Sandvik, M., Rundberget, T., Goldstone, D., Arcus, V., Hovgaard, P., Rise, F., Rehmann, N., Hess, P., Miles, C.O., 2007. Clarification of the C-35 stereochemistries of dinophysistoxin-1 and dinophysistoxin-2 and its consequences for binding to protein phosphatase. Chem. Res. Toxicol. 20, 868–875.

Leal, J.F., Cristiano, M.L.S., 2022. Marine paralytic shellfish toxins: chemical properties, mode of action, newer analogues, and structure–toxicity relationship. Nat. Prod. Rep. 39, 33–57.

Lewis, R.J., Vernoux, J.-P., Brereton, I.M., 1998. Structure of Caribbean ciguatoxin isolated from *Caranx latus*. J. Am. Chem. Soc. 120, 5914–5920.

Loeffler, C.R., Spielmeyer, A., Friedemann, M., Kapp, K., Schwank, U., Kappenstein, O., Bodi, D., 2022. Food safety risk in Germany from mislabeled imported fish: ciguatera outbreak trace-back, toxin elucidation, and public health implications. Front. Mar. Sci. 9.

Mudge, E.M., Meija, J., Uhlig, S., Robertson, A., McCarron, P., Miles, C.O., 2022. Production and stability of oxygen-18 labeled Caribbean ciguatoxins and gambierones. Toxicon 211, 11–20.

Mudge, E.M., Miles, C.O., Ivanova, L., Uhlig, S., James, K.S., Erdner, D.L., Fæste, C.K., McCarron, P., Robertson, A., 2023. Algal ciguatoxin identified as source of ciguatera poisoning in the Caribbean. Chemosphere, 138659.

Murata, M., Legrand, A.M., Ishibashi, Y., Fukui, M., Yasumoto, T., 1990. Structures and configurations of ciguatoxin from the moray eel *Gymnothorax javanicus* and its likely precursor from the dinoflagellate *Gambierdiscus toxicus*. J. Am. Chem. Soc. 112, 4380–4386.

Pottier, I., Vernoux, J.-P., Jones, A., Lewis, R.J., 2002a. Characterisation of multiple Caribbean ciguatoxins and congeners in individual specimens of horse-eye jack (*Caranx latus*) by high-performance liquid chromatography/mass spectrometry. Toxicon 40, 929–939.

Pottier, I., Vernoux, J.P., Jones, A., Lewis, R.J., 2002b. Analysis of toxin profiles in three different fish species causing ciguatera fish poisoning in Guadeloupe, French West Indies. Food Addit. Contam. 19, 1034–1042.

Satake, M., Ishibashi, Y., Legrand, A.-M., Yasumoto, T., 1996. Isolation and structure of ciguatoxin-4A, a new ciguatoxin precursor, from cultures of dinoflagellate *Gambierdiscus toxicus* and parrotfish *Scarus gibbus*. Biosci. Biotechnol. Biochem. 60, 2103–2105.

Satake, M., Murata, M., Yasumoto, T., 1993. The structure of CTX3C, a ciguatoxin congener isolated from cultured *Gambierdiscus toxicus*. Tetrahedron Lett. 34, 1975−1978.

World Health Organization, 2020. Report of the Expert Meeting on Ciguatera Poisoning: Rome, 19−23 November 2018. Food & Agriculture Org. https://apps.who.int/iris/handle/10665/332640. (Accessed 29 September 2023).

Yasumoto, T., Igarashi, T., Legrand, A.-M., Cruchet, P., Chinain, M., Fujita, T., Naoki, H., 2000. Structural elucidation of ciguatoxin congeners by fast-atom bombardment tandem mass spectroscopy. J. Am. Chem. Soc. 122, 4988–4989.